International Journal of Concrete Structures and Materials

RESEARCH Open Access

Dynamic Response Analysis of Coastal Piled Bridge Pier Subjected to Current, Wave and Earthquake Actions with Different Structure Orientations

Riyadh Alsultani[1*], Ibtisam R. Karim[2] and Saleh I. Khassaf[3]

Abstract

The goal of the experiment described in this paper was to examine the effects of structure orientation (0°–90°) and fluid–structure interaction (FSI) under combined water loads, represented by water current and waves, and earthquake actions, on the dynamic response of a reduced-scale bridge pier specimen with pile foundation. The peak relative displacement and peak acceleration of the specimen are measured using the first time innovative in Iraq, Reality Water–Structure–Earthquake Interaction Test (RWSEIT). The findings are given and analyzed concerning water depths, current speed, wave characteristics, earthquake amplitudes, and structural orientations. A numerical model of the examined specimen with three dimensions (3D) was constructed, and the findings were successfully confirmed using the data from the experiments. A pile foundation bridge pier's 3D structural response under orientations that cannot be tested in a lab was computed using the constructed numerical model. The complicated dynamically produced FSI effects on the response of coastal pile foundation bridges may be better understood according to the research's experimental and numerical findings.

Keywords: coastal bridge, pile foundation, structure orientation, dynamic response, fluid–structure interaction, current–wave–earthquake

1 Introduction

Large-span across rivers, seas, straits, or oceans are frequently crossed using pile foundation bridges. Due to their structural efficiency, low cost, and ease of construction, pile foundations have become widely used in deepwater multi-long-span bridges in recent years (AbdelSalam et al., 2010; Wei, 2012). The major component of a bridge's foundation is a collection of long piles that reach the ground below the water's surface and are joined by a substantial concrete cap. The majority of these foundations include pile caps that are partially or completely submerged in the water in addition to the piles, which adds to the consequences of the produced dynamic fluid–structure interaction. Long-span coastal bridges must be built to handle a variety of dynamic stresses, including those brought on by earthquakes, water loads, and traffic (You et al., 2008; Zhang, 2006). When taking into account this type of load, fluid–structure interaction between the vibrating bridge pile foundation and the combined current-wave and earthquake loads is one of the most important considerations. Previous studies on civil engineering structures demonstrated that fluid–structure interaction during earthquakes may change the structural system's dynamic characteristics and result in increased hydrodynamic stresses (Ding

Journal information: ISSN 1976-0485 / eISSN 2234-1315

*Correspondence: reyadabedalabasali93@gmail.com

[1] Department of Construction and Building, Almustaqbal University College, Babil 51001, Iraq
Full list of author information is available at the end of the article

et al., 2015; Huang, 2011; Ji et al., 2019; Liu, 2017; Park et al., 2001; Rajabi et al., 2021; Xiao et al., 2013).

To solve fluid–structure interaction issues involving cylindrical objects submerged in water, such as piles or towers, many analytical methods have been presented (Huang et al., 2022; Jiang et al., 2017; Li & Yang, 2013; Morison et al., 1950; Pang et al., 2015; Wang et al., 2019; Zhang et al., 2019). The original Morison equation (Morison et al., 1950) was used only to calculate the wave force on a pile standing in water. Later, the Morison equation was developed to calculate the earthquake-induced hydrodynamic pressure by Penzien and Kaul (1972). Song et al., (2013) and Yang and Li (2013) expanded the Morison equation to calculate the hydrodynamic pressure during earthquakes for coastal bridges. The results showed that for small-scale piles, namely, slender piles, the viscous effect is important and cannot be ignored, thereupon, the prerequisites of the extended Morison equation are valid. Li et al., (2019) investigated the coefficients in the Morison equation for earthquake-induced hydrodynamic pressure of cylinders. The results indicated that the dynamic characteristics of the pier changed and the seismic response is augmented because of the hydrodynamic pressure effect. The aforementioned analytical dynamic calculations during earthquakes usually assume that the fluid is originally in quiescence without consideration of wave or current motion. Earthquakes, waves, and currents may be simultaneously applied to bridges in the marine environment. Recent incidents involving reinforced concrete bridge collapses have raised awareness of the necessity of performing appropriate maintenance on these important structures. In actuality, the majority of these failures were brought on by improper maintenance intervention scheduling. The steel reinforcement corrosion brought on by the carbonation phenomena is one of the key concerns concerning the load-bearing capability of existing reinforced concrete structures (Crespi et al., 2022). So far, the understanding of the coupling mechanism of multi-disaster loads is not clear enough. At present, there is a limited experimental test, especially for the coexistence field current–wave–earthquake combined flow field. Therefore, the seismic analysis method for pile foundations of sea-crossing bridges is poor, which is a problem that needs to be solved urgently.

Sometimes earthquake forces and water waves can be affected by water currents in one direction. Furthermore, bridges in coastal areas can extend in a longitudinal or transverse direction, and the situation of wave–current and earthquake in a multi-direction may be more dangerous for deepwater bridges. Ding et al., (2018) looked at the pier's dynamic response, conducting a series of scale 50:1 model tests under combined earthquake and wave–current testing. Wave–current action and earthquake excitation were solely taken into account in the longitudinal direction of the bridge during the testing. The structure orientation was not taken into consideration in most of the previous experimental and numerical studies, despite its seriousness. Therefore, it is necessary and urgent need to estimate the accurate impact of this influence on bridges, as they are directly related to people's lives.

The primary goal of this study is to evaluate the dynamic behavior of a pile-supported bridge pier when it is at an angle to the flow direction and is subjected to combined stresses from current–wave action and earthquakes. As a result, the following goals are established: (1) to conduct a new experimental test called the Reality Water–Structure–Earthquake Interaction Test (RWSEIT) to investigate the effects of combined current–wave and earthquake loads with structure orientations (0°, 45°, and 90°); (2) to investigate the dynamic response of reduced-scale bridge pile foundations and discuss the obtained results as a function of current speed, wave properties, earthquake amplitudes, and the structure orientations; (3) Using the validated numerical 3D models to evaluate conditions that cannot be studied in the laboratory, such as a study of the effect of origin when it is at angles of (15°, 30°, 60°, and 75°); and (4) Building three-dimensional (3D) numerical models of the tested specimens, including current–wave–earthquake effects, based on DIANA software. High water loads, earthquakes, and the diffraction of the current, wave, and seismic events are not covered by the paper's scope.

2 Experimental Work

2.1 Test Equipment

A new system illustrated in Fig. 1, called Reality Water–Structure–Earthquake Interaction Test (RWSEIT) the Civil Engineering Laboratory at the University of Technology—Iraq, was specially designed to carry out the dynamic fluid–structure interaction tests on bridge pile foundations. The system is designed to simulate water current, wave, and earthquake action separately or simultaneously in the same system.

As shown in Fig. 1a the test system consists of a wave–current flume with dimensions of $6.0 \times 1.50 \times 1.25$ m, and a horizontal bi-axial shaking actuator below it.

The flume has a flap-style wave maker installed across the tank's width at the upstream end (Fig. 1b). A stepper-controlled electric motor operates the flap. The wave maker can produce both regular and random waves between 0.4 and 1.4 Hz. The maximum wave height is 0.2 m, and the test wave's duration is between 0.5 and 4 s.

Fig. 1 Test system.

The system is also equipped with an electro-mechanical controlled Positive Displacement Pump with three discharge pipes and three suction pipes, their diameters are approximate 19.5 cm. The maximum current speed in the flume can reach 0.5 m/s.

The shaking device located in the middle of the flume can shake in x and y horizontal directions and pitch directions, whose shape is square and dimensions are 1.5×1.5 m. It can be seen from Fig. 1c that the shaking table is with dimensions of 1.0×1.0 m and is connected to the center of the bottom of the water tank using a waterproof cloth. The maximum table load capacity, displacement, acceleration, and frequency are 2 tons, ± 100 mm, 2.0 g, and 40 Hz, respectively. It is worth noting that one of the limitations of the system is that it can test the portable model above the shaking table at angles (0°, 45° and 90°).

At the downstream end of the flume, an inclined mesh plate (Fig. 1d) is fitted to absorb the energy of the oncoming currents–waves and the plate effectively dissipated most of the incoming energy.

2.2 Model Design

The foundation of the continuous bridge crossing the Songhua River in northeast Chin was selected as a case study for the building of the scaled models used in the current study. This foundation is composed of nine circular piles, one square pile cap, and one rectangular pier, in addition to the superstructure of the bridge. The total length of the piles is 58 m, with an assumed segment 12 m above the scour line.

The test model is typically supposed to be a cantilever structure mounted to the top surface of the shaking table to simplify the test plan and theoretical analysis model. With consideration of the superstructure's constraining impact, the lumped mass of the traffic loads and other superstructure components is fixed to the top of the bridge deck.

It is required to create the dynamic similitude relations between prototype and model to replicate the dynamic properties of the prototype structure in the testing. Since the tests primarily examine the individual and combined effects of an earthquake, wave, and current on a bridge

pier, the model's construction must adhere to the laws of similarity between gravity and elastic properties. To simulate the inertial, gravitational, and restoring forces in the tests, it is necessary to concurrently satisfy the Cauchy and Froude scaling criteria, as stated in the following equation:

$$S_L = \frac{S_E}{S_g S_\rho} \tag{1}$$

where S_E is the scale factor of elastic modulus; S_g is the scale factor of gravitational acceleration; S_ρ is the scale factor of density; and S_L is the scale factor of geometry. The scaling factor for the physical quantity S_i in this study is defined as $S_i = i_p/i_m$, where i stands for the physical quantity and the subscripts p and m, respectively, denote the prototype and model. $S_l = 20$ is chosen as an appropriate scale to meet the necessary elastic and geometric similarities by taking into account the dimensions of the Reality Water–Structure–Earthquake Interaction Test (RWSEIT), in regards to the designed flume and shaking table. Table 1 lists the similarities between different physical quantities. Fig. 2 depicts the dimensions of the model inspired by the prototype.

Table 1 Similitude ratios of physical quantities for the dynamic test.

Physical quantity	Scale factor	Value
Length	S_l	20
Area	$S_A = S_l^2$	400
Velocity of flow	$S_u = S_l^{0.5}$	4.47
Quantity of flow	$S_Q = S_l^{2.5}$	1788.8
Elastic modulus	S_E	20
Stiffness	$S_k = S_E S_l$	400
Density	$S_\rho = S_E/S_l$	1
Mass	$S_m = S_\rho S_l^3$	8000
Force	$S_F = S_l^3$	8000
Pressure	$S_P = S_l$	20
Strain	S_ε	1
Stress	$S_\sigma = S_\varepsilon S_E$	20
Displacement	$S_x = S_l$	20
Acceleration	$S_a = S_x/S_t^2$	1
Time	$S_t = (S_m/S_k)^{0.5} = S_l^{0.5}$	4.47
Frequency	$S_f = 1/S_t$	1/4.47

The required model reinforcement areas are adapted according to the similitude requirements tabulated in Table 1, to provide scaled bar yielding force and as presented in the following equation:

$$A_m = \frac{A_P}{S_L^2} = \frac{A_P}{20^2} = 0.0025 A_P \tag{2}$$

where A_m is the tensile stress area of the model reinforcement, A_P is the prototype reinforcement area, and S_L is the length scale factor.

The steel cages, steel spirals, and longitudinal bars of the pile, pier, and cap are prefabricated depending on the

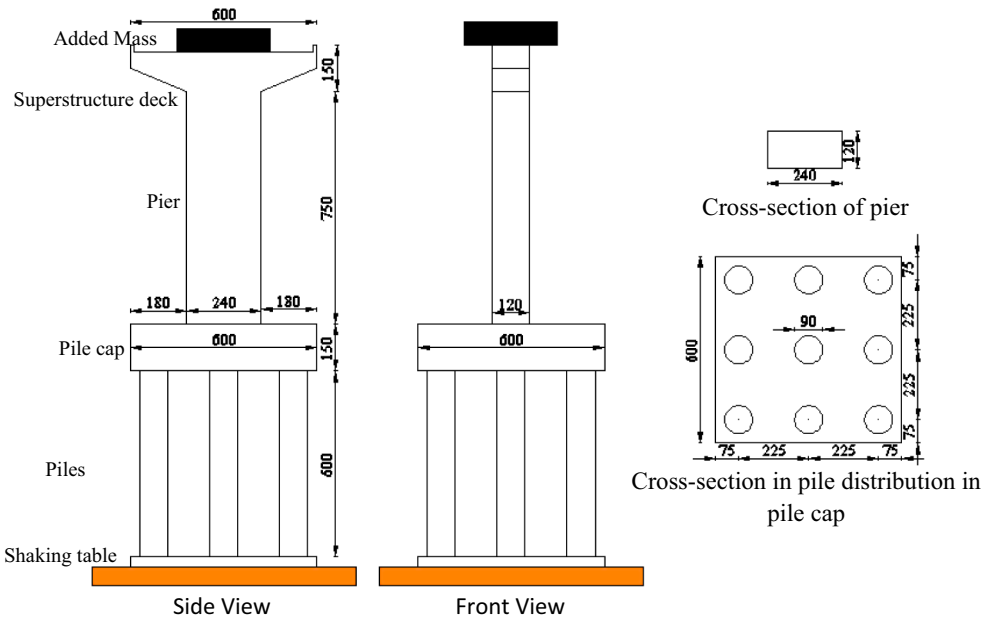

Fig. 2 Dimensions of model that inspired from selected prototype; all dimensions are in (mm).

reinforcement bar details in Fig. 3a, b and c, respectively. The whole model reinforcement is pictured in Fig. 3d.

Fig. 4a, b, and c presents the fabrication procedure of the specimens building that was designed to resemble as closely as possible the construction steps of full-scale bridges.

2.3 Model Calibration

The structure system's displacement and acceleration can show how it responds to dynamic loading. Fig. 5a and b display the comparison curves that emerged between the prototype and the model.

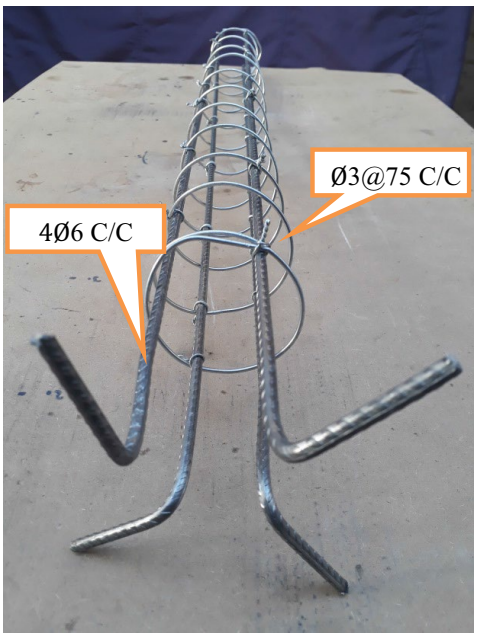

(a) Pile reinforcement.

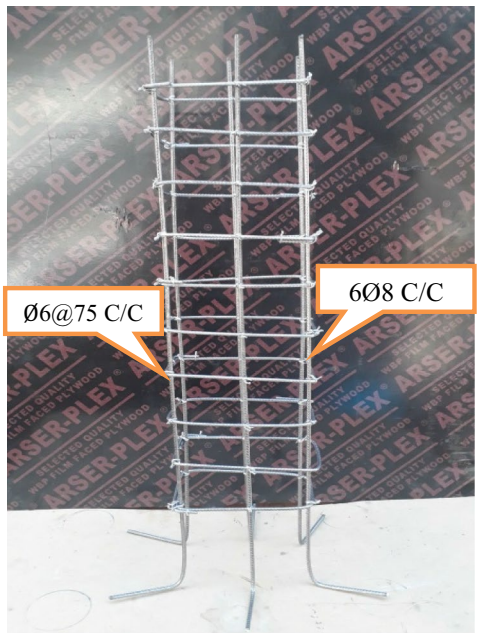

(b) Pier reinforcement.

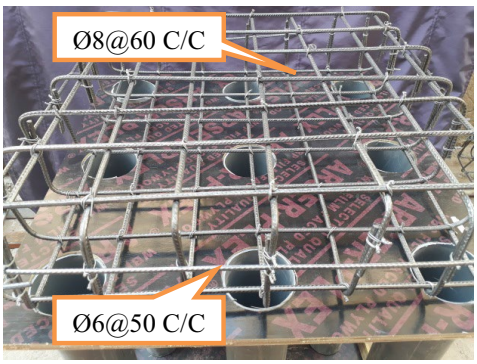

(c) Cap reinforcement.

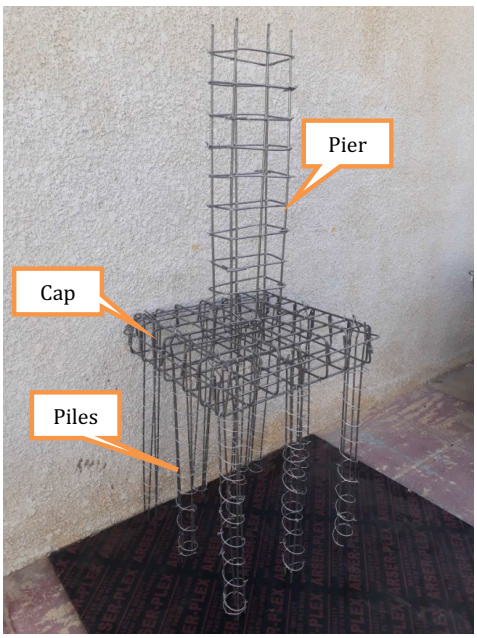

(d)Whole model reinforcement.

Fig. 3 Prefabricated steel of the model reinforcement, all dimensions in (mm).

Fig. 4 Steps of model fabrication. **a** Model timber form. **b** Model concrete casting. **c** Final appearance of the model.

The behavior of the pier top was calculated in the prototype through the use of sensors specialized in calculating displacements, which are (LVDT), and for accelerations, accelerometer sensors were used.

The fact that the prototype and model's response curves nearly match one another demonstrates the applicability of the similitude law in this paper.

2.4 Test Conditions

The specifications of wave amplitude and period with a recurrence time of 50 years were chosen based on field data collected in Iraq. With a length of 2 m and a period of 3 s, the fifth order Stokes wave theory is used. In addition, the analyzed area's current velocity is estimated to be 2 m/s.

The current and wave used in the experiments were uniform current and regular wave, respectively. 0.2 m/sec current speed and the wave properties as period (sec), length (m), and depth (m) i.e. (0.02, 0.1, 2), were designed as test conditions. According to the Chakrabarti, (1987) chart, the current and wave condition is generally considered to be moderate current and short waves, respectively.

Because buckling is more closely related to vertical ground acceleration, it is ignored (Al-Baghdadi, 2014; Hameed, 2019). The ground's pitch motion is less important for the dynamics of maritime constructions than horizontal and vertical motions.

Manjil records are the used earthquake history for the area under study. The peak of time history was taken into account as 1.0 g for the horizontal component following the Iraqi Code of Practice for Seismic Resistant Design of Buildings.

To assess the model structure's response to seismic excitation, the acceleration time record of the Halabjah earthquake, which occurred in Baghdad on November

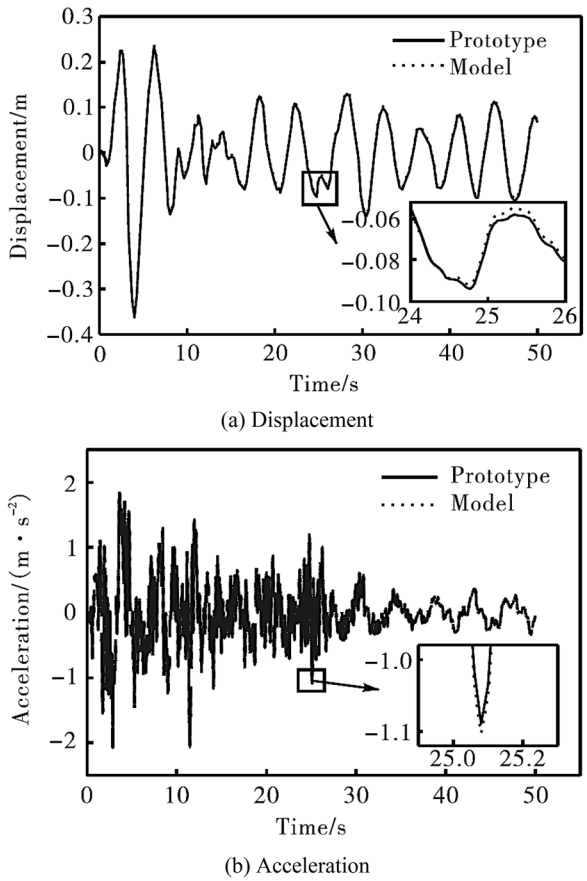

Fig. 5 Comparison of the pier top's displacement and acceleration–time history response curves between the prototype and the model.

12, 2017 (Al-Taie & Albusoda, 2019) was selected as the input earthquake excitation. The original accelerogram has a total ground excitation time history of 205 s with a peak ground acceleration (PGA) of 1.1 g at 41.5 s.

To accomplish these goals with the chosen earthquake, the amplitude was scaled, such that the peak acceleration for the earthquakes is 0.1 g. This earthquake amplitude is representative of minor ground motions, in terms of ensuring structural, not damage. The acceleration period was adjusted permitting to the selected time scale aspect, which is about 45.84 s and as discussed in Table 1 and as in the following:

$$S_t = (S_m/S_k)^{0.5} = S_l^{0.5} = 20^{0.5} = 4.472$$

$$\frac{205}{S_t} = \frac{205}{4.472} = 45.84sec$$

The acceleration time histories for both longitudinal and transverse horizontal components of this scaled earthquake excitation are shown in Fig. 6.

Three water levels (0.60, 0.675, and 0.75) m were taken into consideration in the test, to thoroughly investigate the combined effect of the current, wave, and earthquake on the dynamic response of the pile foundation bridge pier.

To investigate structure orientation effects of the response of pile foundation bridge pier, experiments were conducted when the model is at a certain angle during examination and exposure to combined forces of current–wave and earthquake actions. Angles $\theta 2 = 45^{\circ}$ and $\theta 3 = 90^{\circ}$, were chosen to know the overall behavior when subjected to combined current–wave–earthquake forces, and to compare the behavior they were compared with the angle $\theta 1 = 0^{\circ}$, as pictured in Fig. 7. Peak bridge pier top displacement response relative to the pier bottom and absolute acceleration under combined current wave–earthquake, are tested under three water levels (0.6, 0.675, and 0.75) m. Table 2 lists the test variables that were described earlier.

2.5 Data Acquisition

In design codes and standards, the structural response is frequently considered using the peak analysis of displacement, acceleration, or velocity. The design of marine structures infrequently uses time simulation study of structural response to seismic stimulation. Therefore, four different types of physical variables, including relative displacements and accelerations along the pier height and the characteristics of the currents and waves in the flume, were measured during the testing.

The measurement instruments used to account for these physical values are shown in Table 3. Along the pier, the measurement instruments were distributed uniformly every 150 mm.

3 Numerical Modeling

3.1 DIANA Model

DIANA is a Finite Element Analysis (FEA) solver that does basic and advanced analyses of various structures. DIANA FEA study included modeling the reinforced pile foundation bridge models with the dimensions and characteristics that matched the tested specimens. The geometry has meshed with a set of "controlled mesh": Tetra/Triangle and Hexa/Quad element size limits the possible size between two adjacent elements. Mesh refinement is applied to the whole shape with 0.05 m Hexa/Quad as an element size. The mesh statistics of all models have meshed into 6776–7226 quadrat elements; the number of boundary elements is between 318 and 412.

Rebars which are 3D rods that may be described individually or embedded in oriented surfaces (Al-Khafaji et al., 2021; Mohammed, 2019), are normally used to reinforce concrete constructions; however, in the current

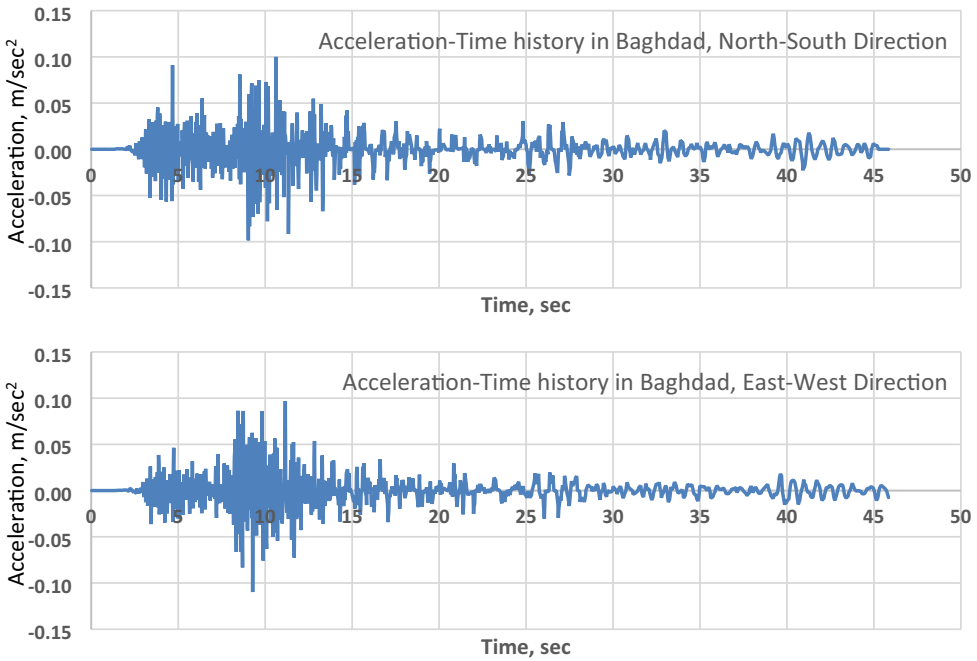

Fig. 6 Scaled acceleration–time history of Halabjah earthquakes.

Fig. 7 Model orientation tests.

Table 2 Present study's test variables.

Water depth (m)		Current speed (m/sec)		Wave properties (m, m, sec)		Earthquake amplitude (*g*)		Structure Orientation (θ)	
H1	0.60	C	0.10	W	0.02, 0.1, 2	E	0.10 g	$\theta 1$	0°
H2	0.675							$\theta 2$	45°
H3	0.75							$\theta 3$	90°

study, the rebar was represented as a solid element, as presented in Fig. 8a. As for concrete materials (Fig. 8b), it has relied on laboratory models in modeling numerical models, in terms of concrete compressive strength, cement quantity, additives materials, slump, and other characteristics (Chun et al., 2022; Kim et al., 2012; Zhao

Table 3 Type, number, and symbol of measuring instruments used in the tests.

Test measures	Instruments	Numbers	Symbol
Displacement	LVDT transducers	8	U
Acceleration	Accelerometer sensor	18	A
Wave properties	Wave gauge	4	–
Flow velocity	current meter	2	–

et al., 2020). The Superstructure and the pier have been modeled using concrete with compressive strength C35 MPa, while the pile cap and the piles were modeled using concrete with compressive strength C30 MPa.

3.2 Load Cases

Boundary conditions must be matched well with the physical conditions of the proper problem. To study the forces that impacted the numerical model, it has been assumed that the pile group is in a state of complete stability, as in the laboratory model, and this procedure was done by choosing Clamped Feet.

The bridges have usually carried a range of forces over their superstructure surface resulting from traffic loads and live load, which was modeled in the laboratory model as Added Mass. To compare the results of the two models, the selected load was spread on the upper surface of the bridge superstructure as Traffic Loads cases.

Earthquake actions were represented as forces affecting the bottom of the model and in both directions (X, Y, or combined of them), just as in the shaking table device in the laboratory system (RWSEIT). DIANA Software allows the possibility of representing the ground acceleration with the values to be shed exactly.

In Fig. 8c, it can be noticed how currents and waves are projected as forces affecting the parts of the numerical model and in the desired direction. This program gives great ease and smoothness to the representation of these forces with the required characteristics.

Mesh refinement is applied to the whole shape with 0.05 m Hexa/Quad as an element size (Fig. 8d). All models contain 6556–7686 quadrat elements in their mesh statistics, and there are between 318 and 412 boundary elements.

4 Test Results and Analysis

4.1 Experimental Results

In the dynamic examination of the bridge pier, the displacement of the pier top relative to the bottom of the pier is the important content of checking the bridge pier's earthquake deformation. The relative displacement of the pier top to the pier bottom is evaluated to assess the structural performance of the bridge pier. The absolute acceleration of the pier top is the most important aspect relating to deck motion under various variables of water levels and loads combined with earthquake action. The peak relative displacement and peak acceleration along the pier were calculated for each 150 mm and as pictured in Fig. 9.

From Figs. 10, 11, and 12, the results showed that the response of the bridge pier for relative peak displacement and peak acceleration of the pier is changed in a very clear way. It can be seen that the water height H2 is distinguished by the increase in dynamic behavior from the other water heights taken in the present study. This is due to the large concrete mass affected by the applied water mass, Where it can be found that the mass of the pile cap is the largest size compared to the other bridge members represented by the pier and the piles.

To analyze these orientations effect, it is clear that the change is increasing the effect of the combined forces with increased direction from 0° to 90°. When the model was at an angle, it makes it more vulnerable to being affected by the forces surrounding it, and this effect may increase when the angle increases from 0° to 45° and increases more when it reaches being at an angle of 90° with the structure.

The peak displacement and acceleration of the pier with direction ($\theta 1$) were 5.475 mm and 0.263 g, while with ($\theta 2$) direction were 7.232 mm and 0.333 g, and with ($\theta 3$) direction were 8.5 mm and 0.379 g. The other conditions of water heights (H1, H2, and H3) are tabulated in Table 4.

It can be concluded that the displacements and the accelerations of the studied variables with directions of 45° and 90° can increases by approximately 32%, 55% for displacement, and 27%, 44% for acceleration, when compared with the behavior of the model with 0° direction.

4.2 Numerical Results

To use the numerical model designed in the present study in tests that cannot be performed in the laboratory; Therefore, a validation of the results of the numerical model was carried out with the results of the test model.

This Software gives great ease and smoothness to the representation of forces with the required characteristics, as indicated in the same, Fig. 6a–e.

The combined test of current–wave–earthquake with 0° structure orientation conducted in the laboratory was verified and the results showed that there is a great agreement between the experimental results (ER) and the numerical results (NR), as shown in Fig. 13.

Furthermore, a series of statistical analyzes were conducted for three laboratory and numerical tests, and

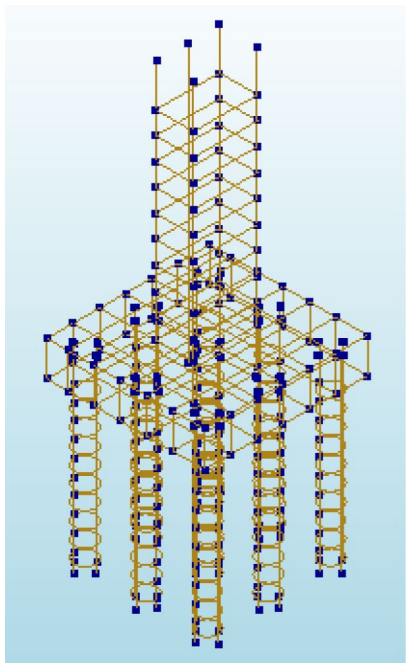

(a) Reinforcement details.

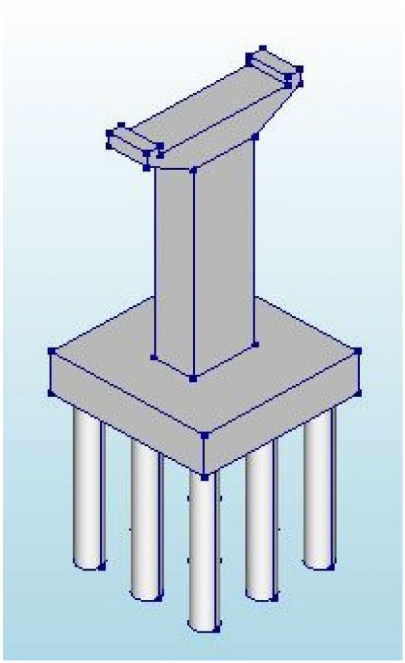

(b) Concrete members.

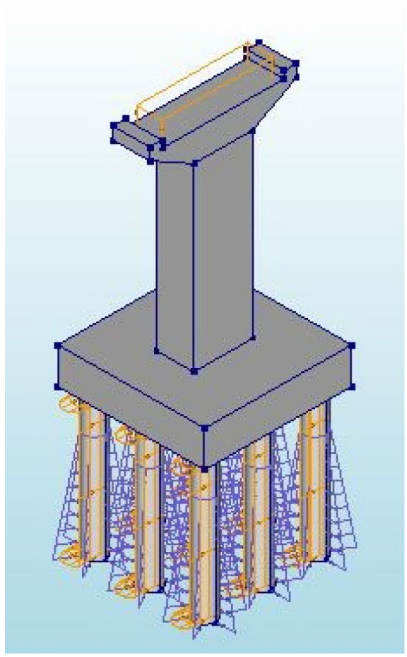

(c) Applied loads.

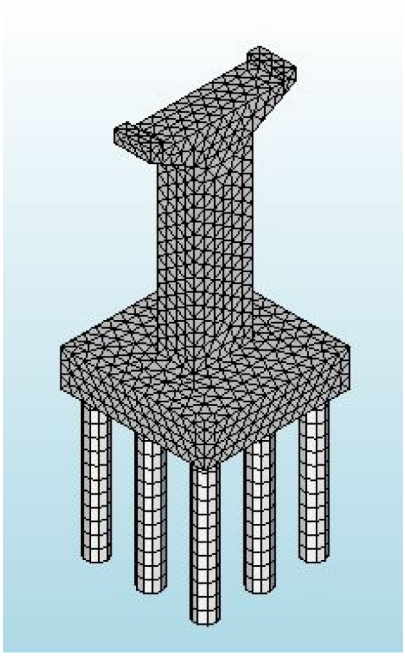

(d) Mesh generation.

Fig. 8 FE model details.

the latest also indicated that there is a great convergence in the results, where the lowest square Regression Coefficient (R^2) is not less than 0.951, while the highest coefficient value reached 0.992. This enables us to say that this model is efficient in conducting other tests that were not performed in the laboratory system (RWSEIT).

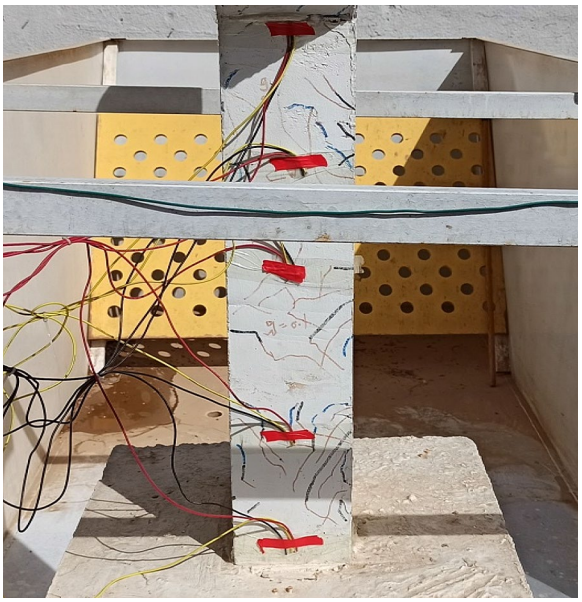

Fig. 9 Displacement and acceleration sensors distribution along pier height.

Since the designed numerical model in this study gives a state of ease and smoothness in shedding the effective forces in different directions, it was proposed to study the structure orientation with a direction that is complementary to those studied in the laboratory, namely, 15°, 30°, 60° and 75°.

From Figs. 14, 15, 16, and 17, it can be shown that the response of the pier increased dynamically when the orientation increases from 15° to 75°. The peak displacement and acceleration of the pier with these complementation directions are tabulated in Table 5. The displacements and the accelerations of the studied variables with directions of 15°, 30°, 60° and 75° can increases by approximately 17%, 22%, 45%, and 47% for displacement, and 15%, 22%, 33%, and 38% for acceleration, when compared with the behavior of the model with 0° direction.

In summary, it can be said that the dynamic behavior of bridges in coastal areas increases significantly with the increase of structure orientation from 0° to 90° and this effect cannot be neglected when designing this type of bridge and under such conditions.

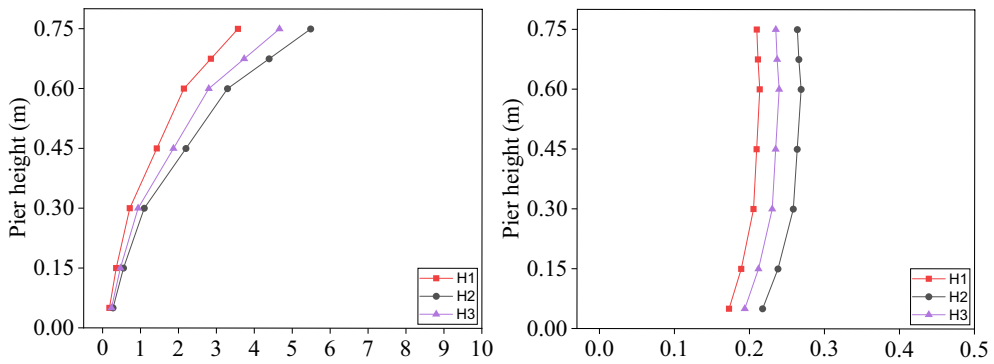

Fig. 10 Peak relative displacement and peak acceleration of the pier under structure orientation (0°).

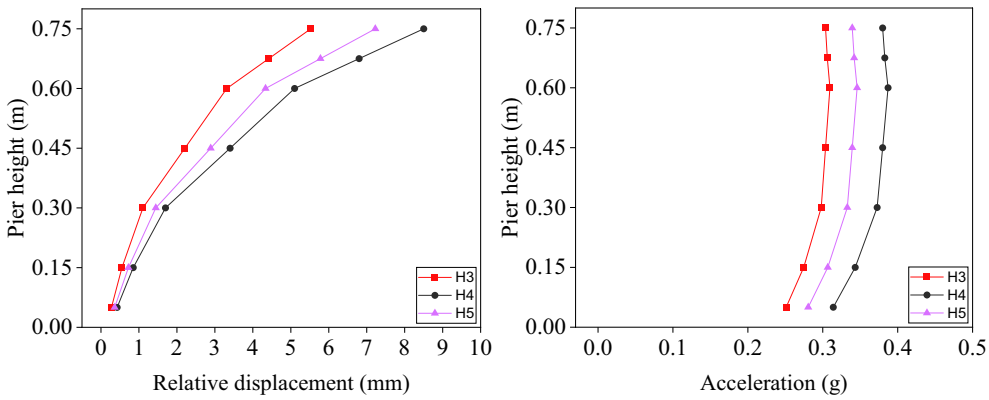

Fig. 11 Peak relative displacement and peak acceleration of the pier under structure orientation (45°).

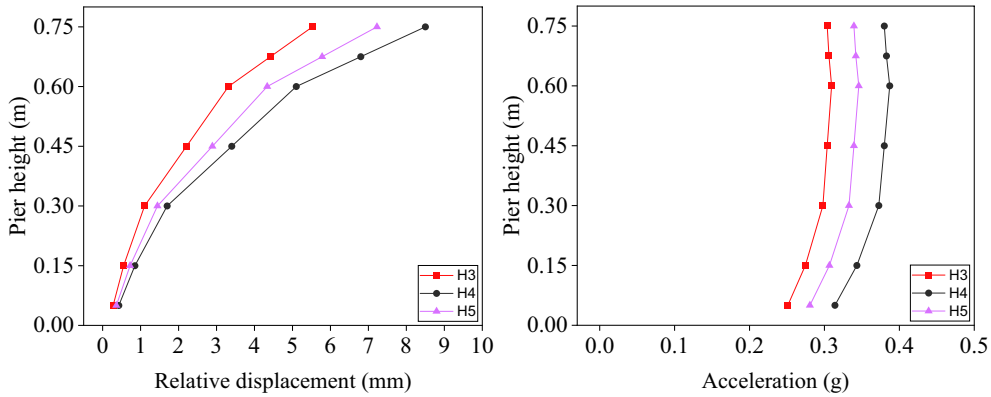

Fig. 12 Peak relative displacement and peak acceleration of the pier under structure orientation (90°).

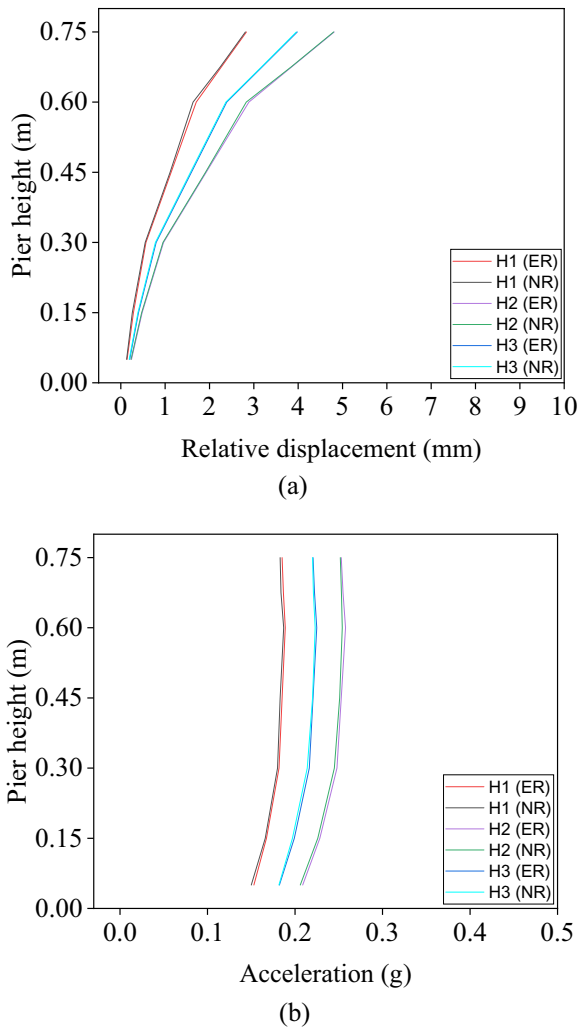

Fig. 13 Experimental results (ER) and Numerical results (NR) under structure orientation (0°).

5 Conclusions

1. The overall dynamic response of the bridge was changed when it was at a certain angle with the applied water forces and earthquake actions. Water height impact at the pile cap is distinguished by the increase in dynamic behavior compared to the pier and the piles.
2. When the model was at an angle, it makes it more vulnerable to being affected by the forces surrounding it, and this effect may increase when the orientation increases from 0° to 90°. Structure orientation increases the dynamic response of the bridge as the direction increases from 0° to 45° and increases more when it reaches being at an angle of 90° with the structure.
3. The peak displacement and acceleration of the pier with direction (0°) were 5.475 mm and 0.263 g, while with (45°) directions were 7.232 mm and 0.333 g, and with (90°) directions were 8.5 mm and 0.379 g, where the displacements and the accelerations of the studied variables with directions of 45° and 90° can increases by approximately 32%, 55% for displacement, and 27%, 44% for acceleration, when compared with the behavior of the model with 0° direction.
4. The peak relative displacement and peak acceleration of the pier with the orientation of 15°, 30°, 60° and 75° was increased by approximately 17%, 22%, 45%, and 47% for displacement, and 15%, 22%, 33%, and 38% for acceleration, when compared with the behavior of the model with 0° direction.
5. The study methodology can be developed to include water loads and earthquakes with high values or directions, to find critical areas that are exposed to

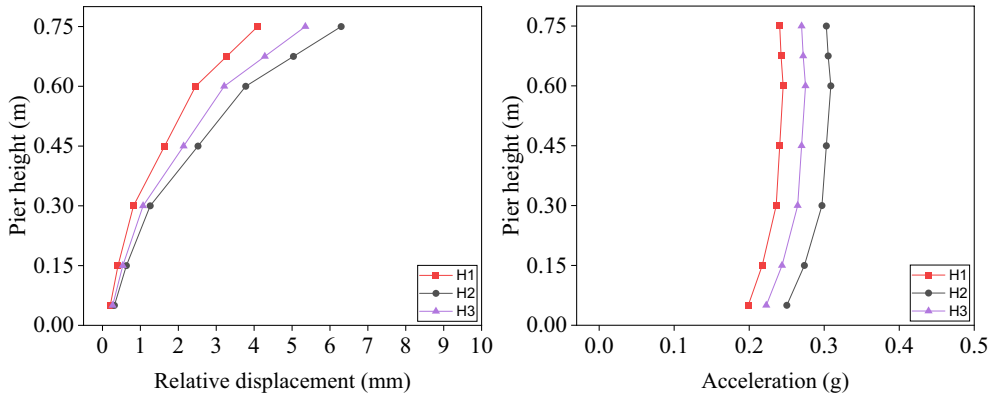

Fig. 14 Peak relative displacement and peak acceleration of the pier under structure orientation (15°).

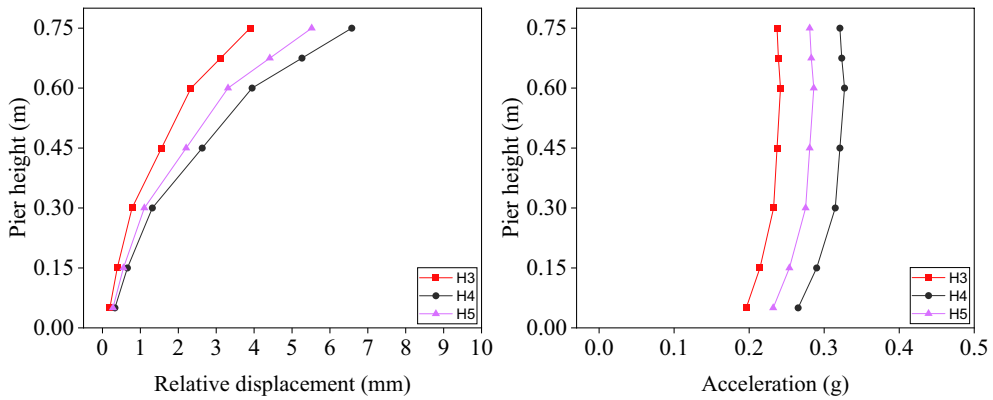

Fig. 15 Peak relative displacement and peak acceleration of the pier under structure orientation (30°).

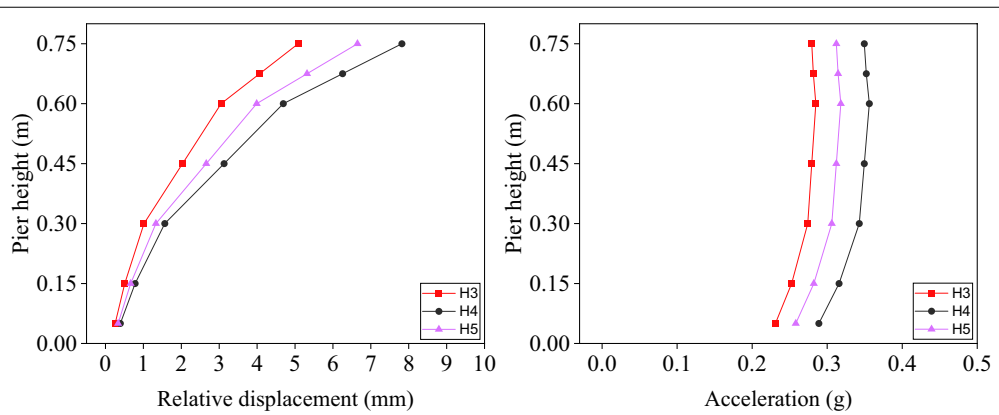

Fig. 16 Peak relative displacement and peak acceleration of the pier under structure orientation (60°).

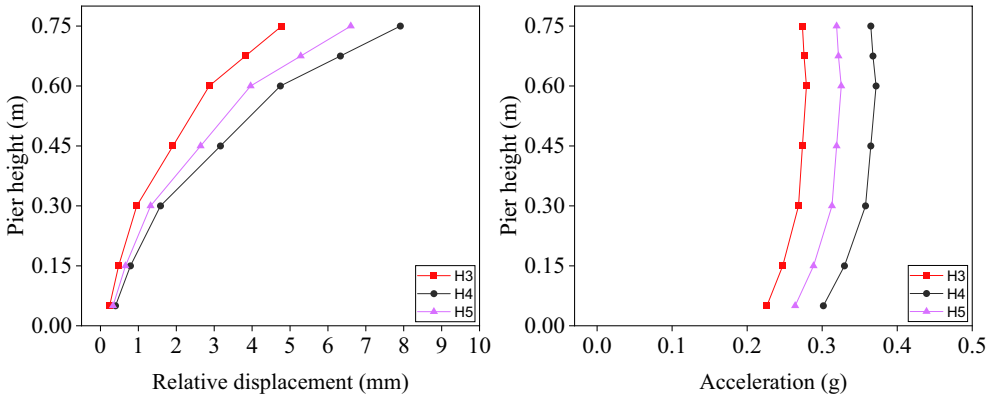

Fig. 17 Peak relative displacement and peak acceleration of the pier under structure orientation (75°).

Table 4 Peak relative displacement and peak acceleration.

Action	H3		H4		H5	
	Disp.	Acc	Disp.	Acc	Disp.	Acc
0°	3.558	0.209	5.475	0.263	4.653	0.234
45°	4.372	0.250	7.232	0.333	6.037	0.291
90°	5.525	0.303	8.500	0.379	7.225	0.400

Table 5 Peak relative displacement and peak acceleration.

Action	H3		H4		H5	
	Disp.	Acc	Disp.	Acc	Disp.	Acc
15°	3.893	0.237	6.296	0.302	5.351	0.269
30°	4.092	0.240	6.576	0.320	5.519	0.280
60°	4.781	0.273	7.821	0.349	6.604	0.312
75°	5.083	0.279	7.911	0.364	6.647	0.319

cracks or damage in such types of marine structures, and then to give another recommendation to the design engineers.

Acknowledgements
Not applicable.

Author contributions
All authors contributed equally to this paper.

Authors' information
Riyadh Alsultani, Ph.D. Student at the University of Technology, Baghdad, Iraq.
Ibtisam R. Karim, Professor Dr at the University of Technology, Baghdad, Iraq.
Saleh I. Khassaf, Professor Dr at the University of Basrah, Basrah, Iraq.

Funding
Not found.

Availability of data and materials
The data and materials had been included in the manuscript.

Declarations

Competing interests
The authors declare that they have no competing interests.

Author details
[1]Department of Construction and Building, Almustaqbal University College, Babil 51001, Iraq. [2]Department of Civil Engineering, University of Technology, Baghdad 10011, Iraq. [3]Department of Civil Engineering, University of Basrah, Basrah 61001, Iraq.

Received: 19 July 2022 Accepted: 16 September 2022
Published: 15 January 2023

References

AbdelSalam, S. S., Sritharan, S., & Suleiman, M. T. (2010). Current design and construction practices of bridge pile foundations with emphasis on implementation of LRFD. *Journal of Bridge Engineering, 15*(6), 749–758.

Al-Baghdadi, H. (2014). Nonlinear dynamic response of reinforced concrete buildings to skew seismic excitation. Ph.D. diss., Ph. D. Thesis, Department of Civil Eng., College of Eng., University of Baghdad.
Al-Khafaji, M. S., Mohammed, A. S., & Salman, M. A. (2021). ANSYS-based structural analysis study of elevated spherical tank exposed to earthquake. *Engineering and Technology Journal, 39*(6), 870–883.
Al-Taie, A. J., & Albusoda, B. S. (2019). Earthquake hazard on Iraqi soil: Halabjah earthquake as a case study. *Geodesy and Geodynamics, 10*(3), 196–204.
Chakrabarti, S. K. (1987). *Hydrodynamics of offshore structures*. Ashurst: WIT press.
Chun, Y., Ryu, E., Lee, Y., Kim, H., & Shin, Y. (2022). Experimental and analytical studies for the size effect on the axial strength of high-strength concrete walls with various fire-damaged areas. *International Journal of Concrete Structures and Materials, 16*(1), 1–14.
Crespi, P., Zucca, M., Valente, M., & Longarini, N. (2022). Influence of corrosion effects on the seismic capacity of existing RC bridges. *Engineering Failure Analysis, 140*, 106546.
Ding, Y., Ma, R., & Li, N. (2015). A simulation model for three-dimensional coupled wave-current flumes. *Eng Mech., 32*(10), 68–74.
Ding, Y., Ma, R., Shi, Y. D., & Li, Z. X. (2018). Underwater shaking table tests on bridge pier under combined earthquake and wave-current action. *Marine Structures, 58*, 301–320.
Hameed, F. (2019). Seismic Behavior of Concrete-Steel Composite Walls. PhD diss., Ph. D. Thesis, Department of Civil Engineering, College of Engineering, University of Al- Nahrain.
Huang, X. (2011). *Mechanism of water-bridge pier dynamic interaction and nonlinear seismic responses of bridges in deep water*. Tianjin: Tianjin Univ. in Chinese.
Huang, Y., Wang, P., Zhao, M., Zhang, C., & Du, X. (2022). *Dynamic response of sea-crossing bridge under combined seismic and wave-current action. Structures*. Amsterdam: Elsevier.
Ji, Z., Fan, L., Zhao, D., Zhu, B., Kang, A., & Li, Z. (2019). Study on computational method of wave force on large-scale rectangular steel boxed cofferdam. *Railway Constr Technol, 36*(3), 1–6.
Jiang, H., Wang, B., Bai, X., Zeng, C., & Zhang, H. (2017). Simplified expression of hydrodynamic pressure on deepwater cylindrical bridge piers during earthquakes. *Journal of Bridge Engineering, 22*(6), 04017014.
Kim, T. H., Seong, D. J., & Shin, H. M. (2012). Seismic performance assessment of hollow reinforced concrete and prestressed concrete bridge columns. *International Journal of Concrete Structures and Materials, 6*(3), 165–176.
Li, Q., & Yang, W. (2013). An improved method of hydrodynamic pressure calculation for circular hollow piers in deep water under earthquake. *Ocean Engineering, 72*, 241–256.
Li, Z. X., Wu, K., Shi, Y., Ning, L., & Yang, D. (2019). Experimental study on the interaction between water and cylindrical structure under earthquake action. *Ocean Engineering*, *188*, 106330.
Liu, L. (2017). Research on computing method of wave-current force on sea-crossing bridge substructures. Southwest Jiaotong Uni., Chengdu.
Mohammed, A. S. (2019). Validation of Finite Element Modeling for Rectangular Reinforced Concrete Beams with Web Openings. *Journal of Engineering and Sustainable Development, 23*(3), 89–98.
Morison, J. R., Johnson, J. W., & Schaaf, S. A. (1950). The force exerted by surface waves on piles. *Journal of Petroleum Technology, 2*, 149–154.
Pang, Y., Kai, W., Yuan, W., & Shen, G. (2015). Effects of dynamic fluid-structure interaction on seismic response of multi-span deep water bridges using fragility function method. *Advances in Structural Engineering., 18*(4), 525–541.
Park, J. C., Kim, M. H., & Miyata, H. (2001). Three-dimensional numerical wave tank simulations on fully nonlinear wave body interactions. *Journal of Marine Science and Technology, 6*(2), 70–82.
Penzien, J., & Kaul, M. K. (1972). Response of offshore towers to strong motion earthquakes. *Earthquake Engineering & Structutre Dynamics, 1*, 55–68.
Rajabi, M., Heydari, F., Ghassemi, H., Ketabdari, M. J., & Ghafari, H. (2021). Three-dimensional numerical modeling of a coastal highway bridge under stokes waves. *Mathematical Problems in Engineering*. https://doi.org/10.1155/2021/8397326
Song, B., Zheng, F., & Li, Y. (2013). Study on a simplified calculation method for hydrodynamic pressure to slender structures under earthquakes. *Journal of Earthquake Engineering, 17*(5), 720–735.
Wang, P., Zhao, M., Du, X., & Liu, J. (2019). Dynamic response of bridge pier under combined earthquake and wave–current action. *Journal of Bridge Engineering, 24*(10), 04019095.
Wei, C. (2012). Numerical simulation of combined actions of wind and wave and their actions on cylindrical component. Harbin Institute of Technology, Harbin.
Xiao, H., Huang, W., Tao, J., & Liu, C. (2013). Numerical modeling of wave forces acting on horizontal cylinder of marine structures by VOF method. *Ocean Engineering, 67*, 58–67.
Yang, W., & Li, Q. (2013). The expanded Morison equation considering inner and outer water hydrodynamic pressure of hollow piers. *Ocean Engineering, 69*, 79–87.
You, Q. Z., He, P., Dong, X. W., Zhang, X. G., & Wu, S. C. (2008). Sutong bridge—the longest cable-stayed bridge in the world. *Structural Engineering International, 18*(4), 390–395.
Zhang, M. (2006). Vibration analysis of solid-fluid interaction for the pier-river water. M.E. thesis, Dalian Jiaotong Univ., Dalian, China.
Zhang, J., Wei, K., Pang, Y., Zhang, M., & Qin, S. (2019). Numerical investigation into hydrodynamic effects on the seismic response of complex hollow bridge pier submerged in reservoir: Case study. *Journal of Bridge Engineering, 24*(2), 05018016.
Zhao, Y., Cao, X., Zhou, Y., Wang, G., & Tian, R. (2020). Lateral load distribution for hollow slab bridge: Field test investigation. *International Journal of Concrete Structures and Materials, 14*(1), 1–13.

Publisher's Note